Title

Chop/Ddit3 depletion in β cells alleviates ER stress and corrects hepatic steatosis in mice

Journal

Science Translational Medicine, 13(604)

ISSN

1946-6234

Authors

Yong, Jing
Parekh, Vishal S
Reilly, Shannon M
et al.

Publication Date

2021-07-28

DOI

10.1126/scitranslmed.aba9796

Peer reviewed

HHS Public Access

Author manuscript

Sci Transl Med. Author manuscript; available in PMC 2022 January 28.

Published in final edited form as:

Sci Transl Med. 2021 July 28; 13(604): . doi:10.1126/scitranslmed.aba9796.

Chop/Ddit3 depletion in β cells alleviates ER stress and corrects hepatic steatosis in mice

Jing Yong[1,*], **Vishal S. Parekh**[2,†], **Shannon M. Reilly**[3], **Jonamani Nayak**[1], **Zhouji Chen**[1], **Cynthia Lebeaupin**[1,3], **Insook Jang**[1], **Jiangwei Zhang**[4], **Thazha P. Prakash**[4], **Hong Sun**[4], **Sue Murray**[4], **Shuling Guo**[4], **Julio E. Ayala**[5,6], **Leslie S. Satin**[2], **Alan R. Saltiel**[3,7], **Randal J. Kaufman**[1,*]

[1]Degenerative Diseases Program, Sanford Burnham Prebys Medical Discovery Institute, 10901 N. Torrey Pines Rd., La Jolla, CA 92037, USA.

[2]Department of Pharmacology, University of Michigan Medical School, 1000 Wall St., Ann Arbor, MI 48105, USA.

[3]Division of Metabolism and Endocrinology, Department of Medicine, University of California San Diego, La Jolla, CA 92093, USA.

[4]Department of Antisense Drug Discovery, Ionis Pharmaceuticals Inc., 2855 Gazelle Court, Carlsbad, CA 92010, USA.

[5]Cardiometabolic Phenotyping Core, Sanford-Burnham Medical Research Institute, 6400 Sanger Road, Orlando, FL 32827, USA.

[6]Department of Molecular Physiology & Biophysics, Vanderbilt University School of Medicine, Nashville, TN 37232, USA.

[7]Department of Pharmacology, University of California San Diego, La Jolla, CA 92093, USA.

Abstract

Type 2 diabetes (T2D) is a metabolic disorder characterized by hyperglycemia, hyperinsulinemia, and insulin resistance (IR). During the early phase of T2D, insulin synthesis and secretion by pancreatic β cells is enhanced, which can lead to proinsulin misfolding that aggravates

*Corresponding author. jyong@sbpdiscovery.org (J.Y.); rkaufman@sbpdiscovery.org (R.J.K.).
†Present address: Chemical Biology and Therapeutics Science Program, Broad Institute, 415 Main Street, Cambridge, MA 02140, USA.

Author contributions: J.Y., V.S.P., S.M.R., T.P.P., S.M., S.G., J.E.A., L.S.S., A.R.S., and R.J.K. conceived and designed the project. J.Y., V.S.P., S.M.R., Z.C., C.L., I.J., J.Z., H.S., S. M., and J.E.A. performed experiments and generated data. J.Y., V.S.P., S.M.R., S.M., J.E.A., L.S.S., A.R.S., and R.J.K. analyzed and interpreted the data. J.Y., V.S.P., S.M.R., and J.E.A. performed statistical analysis. J.N., C.L., and I.J. provided technical support. J.Y., V.S.P. S.M.R., J.E.A., L.S.S., A.R.S., and R.J.K. prepared and revised the manuscript. All authors edited and reviewed the manuscript.

Competing interests: J.Y. and R.J.K. are inventors of a pending U.S. patent titled “Methods and compositions for type 2 diabetes therapy” (U.S. Provisional Application No. 62/933296). The GLP1-ASO compounds targeted to mouse DNA damage inducible transcript 3 (*Ddit3/Chop*) were provided to SBP via a material transfer agreement with Ionis Pharmaceuticals Inc.

Data and materials availability: All data associated with this study are present in the paper or the Supplementary Materials. Raw data are available in data files S1 to S4, which contain raw data for Figs. 1 to 4, respectively. Accession numbers for data deposited into the NCBI Sequence Read Archive are available in table S1.

SUPPLEMENTAL MATERIALS

stm.sciencemag.org/cgi/content/full/13/604/eaba9796/DC1

endoplasmic reticulum (ER) protein homeostasis in β cells. Moreover, increased circulating insulin may contribute to fatty liver disease. Medical interventions aimed at alleviating ER stress in β cells while maintaining optimal insulin secretion are therefore an attractive therapeutic strategy for T2D. Previously, we demonstrated that germline *Chop* gene deletion preserved β cells in high-fat diet (HFD)–fed mice and in leptin receptor–deficient *db/db* mice. In the current study, we further investigated whether targeting *Chop/Ddit3* specifically in murine β cells conferred therapeutic benefits. First, we showed that *Chop* deletion in β cells alleviated β cell ER stress and delayed glucose-stimulated insulin secretion (GSIS) in HFD-fed mice. Second, β cell–specific *Chop* deletion prevented liver steatosis and hepatomegaly in aged HFD-fed mice without affecting basal glucose homeostasis. Third, we provide mechanistic evidence that *Chop* depletion reduces ER Ca^{2+} buffering capacity and modulates glucose-induced islet Ca^{2+} oscillations, leading to transcriptional changes of ER chaperone profile ("ER remodeling"). Last, we demonstrated that a GLP1-conjugated *Chop* antisense oligonucleotide strategy recapitulated the reduction in liver triglycerides and pancreatic insulin content. In summary, our results demonstrate that *Chop* depletion in β cells provides a therapeutic strategy to alleviate dysregulated insulin secretion and consequent fatty liver disease in T2D.

INTRODUCTION

Type 2 diabetes (T2D) is a metabolic disorder that poses a severe health challenge for modern society, as it is estimated by the U.S. Centers for Disease Control and Prevention that 30 million Americans are affected by this condition (1). T2D is characterized by insulin resistance (IR), hyperglycemia, and hyperinsulinemia (2). At the same time, current T2D therapeutics focus on achieving improved blood glucose homeostasis by improving both insulin secretion and reducing peripheral IR. Pharmacological interventions such as glitazones and glucagon-like peptide (GLP1) receptor agonists are limited in that, despite achieving glucose control, there is insufficient clinical evidence to support a beneficial effect on human pancreatic β cells (3).

Pancreatic β cell pathogenesis coupled with peripheral IR has been the traditional explanation for T2D, although recent studies using mouse models and clinical findings made in the Pima Indians (4) support an alternative hypothesis that hyperinsulinemia can serve as a driving force for IR (5, 6). In the Mehran and Johnson paradigm (5), an excessive amount of insulin secreted by pancreatic β cells is the cause of peripheral IR and fatty liver development (7). In this model, reducing the insulin load would therefore alleviate IR. However, experimental observations made using murine *Ins* gene knockout (KO) models may not be relevant to human T2D, although a moderate reduction in insulin production may be beneficial (7). Nevertheless, it is technically challenging to accurately manipulate insulin mRNA abundance (8), especially because it is the most abundant β cell mRNA, accounting for ~30% of the total transcriptome in mature β cells based on our own RNA sequencing (RNA-Seq) data (9) and others' findings (10, 11). Therefore, no current means exist to directly evaluate whether a reduction in insulin expression can achieve beneficial metabolic effects.

On the other hand, previous studies demonstrated that germline deletion of *Chop*, the gene encoding transcription factor C/EBP (CCAAT/enhancer binding protein) homologous protein (also known as *Ddit3/Gadd153*), prevents β cell failure in diabetes models (12-14). It is unknown, however, whether *Chop* deletion protects β cells in a cell-autonomous manner, especially considering the role of CHOP in reducing weight gain (12), regulating hepatic lipid metabolism, and suppressing adipocyte development (12). We therefore generated a conditional *Chop* deletion model to critically evaluate the metabolic consequence of deleting *Chop* in β cells.

RESULTS

Chop deletion in β cells prevents liver triglyceride accumulation in male DIO mice

A conditional *Chop* deletion model was created by breeding a floxed *Ddit3* gene allele (15) with a *RIP-CreERT* transgene (16). In this model, β cell–specific *Chop* deletion is temporally controlled by tamoxifen (TAM) injections (referred to hereafter as "*Chop* βKO" mice; see Table 1 for breeding scheme).

To evaluate the primary effect of *Chop* deletion, we first assessed blood glucose and insulin concentrations in normal diet–fed male *Chop* βKO mice (with TAM administered to 21-week-old mice) compared to the isogenic male littermates that received diluent as controls ($n = 4$ males per group). Four months after *Chop* deletion, *Chop* βKO mice had similar fasting blood glucose concentrations and displayed similar responses to a glucose challenge (intraperitoneally at 1.5 mg glucose per gram weight; Fig. 1A) compared to control littermates. Fasting insulin concentrations were not reduced, whereas glucose-stimulated insulin secretion (GSIS) was blunted at 30 min ($P < 0.05$ for 30 min; Fig. 1B). In addition, we found a trend of reduced β cell function, by applying the homeostasis model assessment of β cell function (HOMA-β) ($P = 0.06$; fig. S1A), but not of HOMA-IR ($P = 0.31$; fig. S1B) (17), suggesting that IR was unchanged in *Chop* βKO mice. Nonetheless, there was a significant linear correlation between fasting insulin and body weight ($P < 0.01$ by F test; Fig. 1C). Furthermore, there was no difference in cumulative weight gain at 4 months in *Chop* βKO mice ($P = 0.11$; Fig. 1D), although reduced weight gain became significant when we included the non-*CreERT* littermates in comparison ($P < 0.05$; fig. S1C). Cumulative weight gain as a function of time was not affected by *CreERT* gene expression, as we previously reported (9).

Aging is a known risk factor for nonalcoholic fatty liver disease (NAFLD) development in humans (18-20) and C57BL/6 mice (21). To test whether pancreatic β cell–specific *Chop* KO was capable of correcting age-associated NAFLD in male mice, we examined another cohort of *Chop* βKO and wild-type (WT) littermates, sacrificed at 11, 14, and 17 months of age. Pancreatic β cell–specific *Chop* KO was mediated by TAM injections at 5 months before sacrifice, whereas the isogenic littermates received phosphate-buffered saline (PBS) as controls. Mice gained weight during aging, and *Chop* βKO had minimal effect on cumulative weight gain [$P < 0.05$ by two-way analysis of variance (ANOVA) but not by post hoc t test; fig. S2]. Consistent with a previous report (21), aging (with normal diet feeding) caused liver fat accumulation in mice sacrificed at 14 and 17 months of age, as evidenced by hematoxylin and eosin staining of enlarged hepatocytes, increased oil red O

staining (fig. S3A), and increased liver weight ($P < 0.05$ by two-way ANOVA; fig. S3B). In contrast, *Chop* βKO mice displayed reduced fasting serum insulin concentrations that correlated with reduced NAFLD in aged mice, as reflected by normal-sized hepatocytes (fig. S3A) and decreased liver weight ($P < 0.05$ by two-way ANOVA; fig. S3B). Last, pancreatic β cell–specific *Chop* KO significantly reduced triglyceride (TG) content in aged mouse livers ($P < 0.01$ by *t* test; fig. S3C), supporting the notion that *Chop* KO in β cells corrected aging-induced NAFLD.

Because diet-induced obesity (DIO) is a known risk factor for NAFLD, we tested whether *Chop* KO in β cells could correct DIO-induced NAFLD. Mice were challenged with a high-fat diet (HFD; 45% fat in kcal) for 20 weeks, starting at 9 weeks of age, with *Chop* deletion induced by TAM at 10 weeks of HFD feeding (Fig. 1E). In addition, we selected littermates harboring WT *Chop* alleles as a TAM-treated control group. Before *Chop* deletion, the two groups were metabolically indistinguishable with no significant difference in body weight or blood glucose concentrations, either before or after 10 weeks of HFD (Fig. 1, F and G). After *Chop* deletion, a moderate but significant decrease in body weight was observed in *Chop* βKO mice ($P < 0.01$ at week 20; Fig. 1F), which had no effect on blood glucose (Fig. 1G). After 20 weeks of HFD feeding, murine livers were dissected for visual inspection and liver TG analysis. HFD feeding caused hepatomegaly and liver discoloration associated with fatty deposits in control littermates (Fig. 1H) as well as for a *Chop* β heterozygous (βHet) mouse in the litter (Fig. 1H). In contrast, the three *Chop* βKO mice had normal-sized livers and appeared healthy (Fig. 1H). The morphological impression was further confirmed quantitatively by significantly reduced liver weight and TG content in *Chop* βKO mice compared to littermates ($P < 0.05$ for both; Fig. 1, I and J). We surmised that chronically reduced β cell insulin secretion may prevent fatty liver development in the HFD-fed C57BL/6 mice, as previously proposed by others (5, 6). Supporting this hypothesis, pancreatic insulin content (standardized by tissue wet weight) in the *Chop* βKO mice was not different ($P = 0.11$; Fig. 1K), which nonetheless positively correlated with TG content ($P < 0.05$ by *F* test; Fig. 1L). Consistent with a recent report that demonstrated IR as a causal factor for hepatic de novo lipogenesis in human NAFLD (7), it will be of interest to investigate whether the reduced fatty liver that we observed here reflects reduced de novo hepatic lipogenesis or increased export from hepatocytes or fatty acid oxidation.

Chop deletion in β cells improves insulin secretion under glucose clamp without altering general glucose metabolism

Observing the blunted GSIS response and the protection from HFD-induced hepatic steatosis in the *Chop* βKO mice, we further investigated whether the reduced pancreatic insulin content negatively affected general glucose metabolism. For this purpose, a follow-up 22-week HFD experiment was performed using male mice, during which body weight, food intake, and nonfasting blood glucose were monitored. We found no significant differences in these variables at any time point when comparing *Chop* βKO to their *Chop* βHet littermates (Fig. 2, A to C, respectively), whereas glucose tolerance in all the HFD-fed mice exhibited a significantly increased glucose excursion from baseline regardless of *Chop* status [area under the curve–intraperitoneal glucose tolerance test (AUC-IPGTT); *P*

= 0.0001 by two-way repeated-measures (RM)–ANOVA and $P = 0.88$ for *Chop*; Fig. 2D]. Comparison of IPGTT curves also revealed no difference at every time point, confirming that the blunted GSIS response in *Chop* βKO mice did not cause glucose intolerance (fig. S4). In the same experiment, *Chop* βKO HFD mice were similarly sensitive to insulin after 18 weeks of HFD feeding (with TAM administered at 8 weeks after initiation of HFD; compare fig. S5, A and B). Consistent with the insulin measurements made in mice fed normal diet (Fig. 1B), *Chop* βKO HFD-fed mice had similar serum C-peptide compared to *Chop* βHet littermates, both before and after glucose stimulation (fig. S5C). Furthermore, in another independent cohort where *Chop* was deleted by TAM before HFD feeding, there was no difference in blood glucose or free fatty acid concentrations in response to a bolus of insulin injection between *Chop* βKO mice and their littermates, either on normal chow or HFD (fig. S6), confirming that insulin sensitivity did not change in *Chop* βKO mice.

Because we observed no adverse effects of *Chop* deletion on mouse whole-body metabolism, we performed a hyperglycemic clamp test on a different HFD-fed cohort using *Chop* βKO mice of both sexes (Fig. 2E) again using age-matched *Chop* βHet littermates as controls. Although no differences were observed in body weight or fasting blood glucose (Table 2), both insulin and C-peptide secretion in *Chop* βKO mice were significantly slowed after hyperglycemia clamping, with delayed, increased secretion of both after 40 min ($P \leq 0.01$ by two-way RM-ANOVA; Fig. 2, F and H). The control *Chop* βHet mice showed basal hyperinsulinemia and reduced first-phase responses to glucose, demonstrating that the HFD model properly replicated the phenotype of humans during the prediabetic and early T2D phases. *Chop* βKO mice required a significantly higher glucose infusion rate (GIR) to maintain their blood glucose target at ~300 mg/dl (=16.7 mM; Fig. 2G) ($P = 0.0001$; Fig. 2I), suggesting that the increased glucose clearance was due to increased insulin secretion and not altered insulin sensitivity ($P = 0.82$; Fig. 2J). Similar to the normal diet–fed cohort (fig. S1, A and B), there was a significant difference in β cell function defined by HOMA-β ($P < 0.05$; fig. S7A), whereas there was no difference in HOMA-IR ($P = 0.68$; fig. S7B). Furthermore, the differences found in the hyperglycemic clamp study were not due to altered β cell mass of the *Chop* βKO mice, because no statistical significance was found in the fractional insulin immunopositive (insulin$^+$) areas (with representative islet morphologies shown in fig. S8 and the total surveyed pancreata areas reported in fig. S9A; Fig. 2K). Similarly, no differences were observed in the two groups with regard to α cell distribution in the islets (fig. S8, B versus D), α cell mass, or the relative ratio of α cells to α cells (fig. S9, B to D). To investigate whether the in vivo effect of β cell–specific *Chop* KO was associated with altered β cell turnover in islets, such as cell proliferation (using the proliferating cell antigen Ki67 as a marker) or apoptosis [using terminal deoxynucleotidyl transferase–mediated deoxyuridine triphosphate nick end labeling (TUNEL) as a marker; fig. S10A], we stained pancreas sections from aged *Chop* βWT and *Chop* βKO male mice sacrificed at 11 months of age and found no change in the percentage of Ki67$^+$ or TUNEL$^+$ within the pancreatic β cell population (fig. S10, B to D). Consistent with the large body of experimental evidence that suggests that there is either low or no pancreatic β cell turnover in islets of humans (22) and in adult mice (23, 24), there was generally a low number of both Ki67$^+$ and TUNEL$^+$ cells among pancreatic β cells in *Chop* βKO mice and in littermates. Electron microscopy also revealed no gross changes in insulin granule density or

ER morphology ER in *Chop* βKO islets (fig. S11). Last, we ruled out the possibility of an indirect effect of β cell *Chop* deletion on hepatic gluconeogenesis using a pyruvate tolerance test (fig. S12).

Furthermore, correction of hyperinsulinemia is often associated with metabolic fitness in general (25, 26). To evaluate whether *Chop* KO in β cells also conferred general metabolic fitness in these animals beyond correcting hepatic steatosis, we measured the metabolic rate of *Chop* βKO mice using metabolic cages. Consistent with the notion that correcting hyperinsulinemia confers resistance to metabolic abnormalities caused by aging and obesity, oxygen consumption rates (VO_2) and carbon dioxide production rates (VCO_2) were significantly higher in KO animals ($P = 0.02$ for both parameters; fig. S13A), although these values did not reach significance after body weight normalization with a boundary P value (fig. S13B). These findings indicate that *Chop* βKO mice displayed a beneficial increase in energy expenditure and heat production compared to WT mice ($P = 0.02$; fig. S13C). There was no difference in respiratory exchange ratio (fig. S13D), indicating that there was no change in substrate utilization (carbohydrate versus fat catabolism). Last, there were no significant changes in food or water intake between genotypes. Circadian rhythm is known to regulate feeding behavior, and correctly timed feeding is associated with metabolic health and longevity (27). The pattern of food and water consumptions suggests that Chop βKO mice may be protected from obesity-associated circadian rhythm dysregulation (fig. S13, E and F). In addition, there was a slight increase in total body fat in *Chop* βKO mice ($P = 0.04$; fig. S14A), suggesting a metabolically healthy distribution of body fat, favoring adipose tissue storage over metabolically harmful ectopic lipid deposition (fig. S14B).

Chop deletion in β cells reduces insulin transcripts and ER stress in male DIO mice

To confirm that *Chop* deletion in β cells reduces ER stress (12), we performed molecular analysis of unfolded protein response (UPR) markers using quantitative reverse transcription polymerase chain reaction (qRT-PCR) and subsequently whole transcriptomic profiling by RNA-Seq (9, 28) on RNA extracted from the islets of male HFD-fed mice. Molecular assays revealed greatly decreased insulin-encoding transcripts for both *Ins1* and *Ins2* (~75% reduction in *Chop* βKO islets; Fig. 3A) associated with reduced UPR markers, for example, *Atf4, Bip,* and spliced *Xbp1* (*sXbp1*), in βKO islets compared to βWT littermates (Fig. 3B). Furthermore, supporting our findings by qRT-PCR, transcriptome profiling showed a significant reduction in other UPR markers, represented by *Atf3, Bip/Hspa5, Sec23b,* and *ERdj4/Dnajb9* ($P < 0.05$; Fig. 3C). *Chop* deletion did not affect β cell identity, because key β cell transcription factors including *Pdx1, Nkx6.1, Mafa, Isl1,* and *Ngn3* were not altered in *Chop* βKO islets (Fig. 3D), consistent with our histological findings of unchanged β cell mass and islet morphology. In addition, *Chop* deletion did not alter the abundance of mRNAs encoding *Cpe, Glut2,* or *PC1/2* (fig. S15), further supporting the hypothesis that *Chop* deletion did not impair β cell differentiation status. In contrast, *Wfs1, Gadd34/Ppp1r15a,* and *Bip/Hspa5* (encoded by two alternatively spliced isoforms, namely, *NM_022310* and *NM_001163434*), representing the UPR target genes for the IRE1α, PERK, and ATF6 branches of the UPR, respectively, were all significantly reduced except for *Gadd34* ($P \leq 0.05$; Fig. 3E). Reductions in UPR transcript abundance were supported further by our finding that a subset of mRNAs that encode ER proteins were

altered (Fig. 3F), suggesting that CHOP has a long-term effect on ER remodeling. Because the UPR is an adaptive response to ER stress, we biochemically tested whether *Chop*-deleted β cells exhibited reduced ER stress by probing the interaction between proinsulin and BiP (binding immunoglobulin protein). BiP binding to misfolded proinsulin is the gold standard biochemical indicator for proinsulin misfolding in β cells (29-31). By BiP coimmunoprecipitation (co-IP) assay, we confirmed that less BiP protein was associated with proinsulin in the *Chop* βKO islets (Fig. 3G) compared to βHet islets, consistent with reduced ER stress in *Chop* βKO islets. Furthermore, to investigate whether the altered insulin secretion in response to the hyperglycemic clamp was an islet-autonomous effect, we isolated islets from a batch of lean *Chop* βKO mice and their age-matched littermates (*Chop* βHet mice) and performed an in vitro GSIS assay along with metabolic pulse-chase labeling of nascent proinsulin using ^{35}S-methione + ^{35}S-cysteine to track the intracellular proinsulin processing. Fully supporting the in vivo clamp study, *Chop* βKO islets displayed a delayed, increased insulin secretion dynamics, evidenced by the cumulative insulin secretion into the conditioned media (Fig. 3H). Specifically, although there was a discernible reduction in insulin release from *Chop*-null islets at 1 hour after 16.7 mM glucose stimulation, prolonged incubation of the islets in glucose for 2 hours stimulated a greater amount of insulin secretion from βKO islets (Fig. 3H) compared to βHet islets. In the same experiment, pulse-chase labeling with ^{35}S-Met/^{35}S-Cys also suggested that the nascent proinsulin molecules were less retained in the *Chop* βKO islets at the end of the 2-hour chase period (Fig. 3I). Scintillation quantification independently confirmed that there was proportionally less retained ^{35}S radioactivity in the *Chop* βKO islets (Fig. 3J) compared to βHet islets, with the assumption that most of the reduced ^{35}S radioactivity reflects secretion of newly synthesized insulin. Theoretically, newly synthesized insulin contributes proportionally more to the second phase of insulin release from β cells (32). In conclusion, the in vitro GSIS assay performed on isolated islets reproduced the in vivo insulin secretion pattern revealed by hyperglycemic clamp, thereby providing a potential mechanism of action for in vivo insulin reduction and hyperinsulinemia correction. Collectively, these results led us to hypothesize that, under physiological conditions, CHOP serves as a transcriptional hub in β cells that can alter ER function by increasing the expression of genes encoding ER structural, ER functional, and ER-to-Golgi trafficking proteins to accommodate proinsulin synthesis (fig. S18). Conversely, *Chop* deletion in β cells decreased proinsulin mRNA accompanied by more efficient folding as indicated by faster proinsulin processing and less BiP interaction due to reduced ER stress.

ER stress up-regulates insulin mRNAs, and GLP1-*Chop* ASO corrects liver TG accumulation

A missing mechanistic link, however, is that CHOP does not directly bind to the promoter regions of all of these affected genes (Fig. 3F), as we demonstrated previously using chromatin IP sequencing (ChIP-Seq) (28). Thus, we wondered how *Chop* deletion could result in changes in ER function without altering the promoter activity of ER-related genes. The ER is the major intracellular Ca^{2+} storage organelle, and both ER and cytosolic Ca^{2+} as well as adenosine 5′-triphosphate (ATP)–to–adenosine 5′-diphosphate (ADP) ratios can be profoundly affected by physiological ER stress (33, 34). Ca^{2+} has a crucial physiological role in pancreatic islets, because glucose-dependent cytosolic Ca^{2+} oscillations driven by

membrane electrical activity trigger insulin exocytosis (35-37) and *Ins* gene transcription is positively regulated by cytosolic Ca^{2+} concentrations (38, 39). We therefore tested whether the *Chop* deletion–dependent changes in islets were associated with altered ER Ca^{2+} signaling, representing a logical outcome from reduced ER stress.

For this purpose, we tested the effect of a membrane-permeable intracellular Ca^{2+} chelator, BAPTA-AM [1,2-bis(2-aminophenoxy) ethane-*N,N,N′,N′*-tetraacetic acid acetoxymethyl ester] (abbreviated as "BAPTA" hereafter), on islets isolated from C57BL/6 mice. When islets were exposed overnight to BAPTA (10 μM), we observed reductions in both *Ins1* and *Ins2* mRNA (Fig. 4A). At the same time, *Chop* and *sXbp1* abundance were also reduced by BAPTA treatment, suggesting that lowering β cell Ca^{2+} reduced UPR induction in these WT islets, possibly by decreasing the proinsulin translation burden placed on the ER (Fig. 4A). Tunicamycin (Tm; 0.5 μg/ml), in combination with BAPTA treatment, rescued the decrease in both *Ins1* and *Ins2* mRNA abundance, showing that the effect of Ca^{2+} chelation on β cell ER stress could be overcome by pharmacological ER stress induction, indicating that ER stress induction of *Ins* mRNA expression involves other factors independent of Ca^{2+} signaling. Concomitantly, *Chop* and *sXbp1* mRNAs, as well as *BiP* mRNA were induced by Tm treatment (BAPTA columns versus BAPTA + Tm columns; Fig. 4A).

The previously reported positive regulation of *Ins1/Ins2* transcription by ER stress (9) was further confirmed in a separate batch of *WT* and *Chop* βKO islets treated with Tm (5 μg/ml) (fig. S16). In contrast, induction of *Chop* mRNA by activating GCN2 using halofuginone (HFn; 50 nM), a potent transfer RNA (tRNA) synthetase inhibitor (40, 41) to induce eIF2α phosphorylation, reduced *Ins1* and *Ins2* transcripts, as well as sXBP1, despite pronounced *Atf4* and *Chop* induction (Fig. 4A). Under HFn treatment, *Chop* induction is partially attributable to the amino acid response element sequence in the *Chop* promoter (42). Last, addition of cyclosporine A (CsA; 200 nM) to islet media induced both *Ins1* and *Ins2* transcripts, suggesting that the ER Ca^{2+} effect on *Ins1/Ins2* expression was unlikely due to a direct consequence of activation of the calcineurin/NFAT (nuclear factor of activated T cells) pathway (43) by Ca^{2+}.

Insulin granule secretion from mature β cells is dependent on cytosolic Ca^{2+} oscillations, and *Chop* βKO islets exhibited reduced cytosolic Ca^{2+} concentration in response to 11 mM glucose ($P < 0.0001$; Fig. 4B). ER Ca^{2+} content was also reduced in these islets (Fig. 4C). Furthermore, GLP1-conjugated antisense oligonucleotides (GLP1-ASOs) demonstrated efficient gene knockdown in rodent islets (44), providing an attractive, independent strategy to mediate *Chop* knockdown to test our hypothesis. We therefore treated mice with floxed *Chop* alleles (15) (on the *C57BL/6* background without *CreERT*) with GLP1-*Chop* ASO in vivo (Fig. 4D) by subcutaneous injections in young mice of both sexes. Control group of littermates received GLP1-conjugated control ASO (a sequence not homologous to any known gene in the murine genome). As expected, GLP1-*Chop*-ASO administration was well tolerated by the mice and specifically reduced islet *Chop* transcripts by >60% (Fig. 4E), with minimal effects on other C/EBP family members (*Cebpa, Cebpb,* and *Cebpg*) in either islets or liver tissue, demonstrating β cell selectivity as reported (44). Further supporting our hypothesis, treatment with GLP1-*Chop*-ASO reduced the ER Ca^{2+} pool without secondarily affecting the relative cytosolic Ca^{2+} concentrations stimulated by 11 mM glucose (Fig.

4, F and G), suggesting that the change in ER Ca^{2+} was a primary event immediately after *Chop* knockdown. This is proof of principle that the GLP1-ASO strategy can be exploited to alter islet physiology and Ca^{2+} dynamics. These results support our working hypothesis featuring an ER-centric role of CHOP in pancreatic β cells (fig. S18). Because GLP1-*Chop* ASO–treated islets displayed ER Ca^{2+} changes analogous to *Chop* βKO islets, we investigated whether GLP1-*Chop* ASO also reduced liver TGs analogous to the *Chop* βKO mice. We tested GLP1-*Chop* ASO in two widely used murine NAFLD models. For the DIO model, male *C57Bl/6* mice received 10 weekly GLP1-*Chop* ASO (1 mg/kg per week), GLP1-scrambled ASO (1 mg/kg per week), or unconjugated *Chop* ASO doses (0.5 mg/kg per week), starting from 12 weeks after 45% HFD initiation (22 weeks total of HFD). For the $Lpr^{db/db}$ model, male $Lpr^{db/db}$ mice received eight weekly GLP1-*Chop* ASO (3.2 mg/kg per week), GLP1-scrambled ASO (3.2 mg/kg per week), or unconjugated *Chop* ASO (1.6 mg/kg per week) doses, starting from 5 weeks of age with standard diet (Fig. 4H). GLP1-*Chop* ASO–treated mice had reduced liver TGs, which became significant when the two control groups were pooled for comparison with GLP1-*Chop* ASO group ($P < 0.05$; Fig. 4I), and significantly reduced pancreatic insulin ($P < 0.05$; fig. S17, A and B), without an effect on their body weight (fig. S17, C and D). In summary, analogous to *Chop* βKO, *Chop* GLP1-*Chop* ASO dosing reduced liver TGs in orthogonal NAFLD models, apparently as a result of reduced pancreas insulin but not of reduced body weight.

DISCUSSION

In summary, we propose that CHOP is activated by UPR signaling through the PERK branch, as a response to increased proinsulin synthesis and misfolding (45). In turn, CHOP serves as a transcriptional hub to maintain ER proteostasis. This process also controls insulin transcription, partially via Ca^{2+} signaling, from the ER to the nucleus, although this is unlikely directly mediated by CHOP. Furthermore, ER remodeling, in turn, has a profound effect on ER Ca^{2+} that subsequently regulates the increase in cytosolic Ca^{2+} that occurs in response to elevated glucose. At the same time, comparison of the genetic *Chop* βKO model versus the GLP1-ASO–mediated *Chop* knockdown model demonstrated that the *Chop* deletion–induced GSIS change is a chronic complex event in β cells, with the ER Ca^{2+} pool change preceding the insulin mRNA reduction and GSIS decrease.

Because the pancreatic islet is a nutrient sensing organ and β cells secrete insulin to increase anabolic metabolism upon nutrient availability, we speculate that, when there is a surfeit of nutrition, increased insulin secreted into the circulation exacerbates IR and promotes fatty liver in humans (7), although there was a dissociation between HOMA-IR (17) and hyperinsulinemia in *Chop* βKO mice. We were initially intrigued to find that a 75% reduction in *Ins1 and Ins2* mRNA by *Chop* deletion did not produce a strong metabolic phenotype in mice, although this was not unprecedented (5, 6, 11). Insulin mRNA may be in excess in β cells and crucial for glucose sensing. This may be better explained by a model proposing that ER stress due to increased proinsulin synthesis is coupled to insulin secretion, mediated through an ER Ca^{2+} response in β cells. In the UPR signaling cascade, however, *Perk* deletion (46), eIF2α phosphorylation site mutation (47, 48), *Ire1*α deletion (9), *sXbp1* deletion (49), and *Atf6* deletion (50) all caused deleterious outcomes in β cells and were thus unsuitable therapeutic targets. *Chop* deletion may be the only example that can safely

reduce ER stress in β cells (12) by exemplifying a “thrifty gene” providing an evolutionary advantage during famine (51). This hypothesis is more attractive, given our finding that β cell–specific *Chop* deletion prevented HFD-induced hepatic steatosis, echoing recent human findings (7).

Despite the profound changes in insulin secretion induced by *Chop* deletion (via the genetic *CreERT-LoxP* system) and the subsequent pronounced reduction in liver TG, such a murine model has limitations. First, the selected transgene combination determined by Mendelian ratio governs the experimental animal yield (Table 1), which is not particularly high, considering the typical C57BL/6J litter size. Therefore, at any given time, only a small number of experimental and control animals are available for direct comparison. In addition, we determined that it is essential to compare littermates for a robust analysis. Second, measurements of insulin concentrations in blood are inherently “noisy,” and insulin concentrations sampled from peripheral blood are an approximation of direct insulin secretion, with liver filtration and clearance as main complexing factors (52). Addressing these limitations would require further experiments. Alternative experimental procedures, such as blood sampling directly from the portal vein while animals are maintained under normal feeding conditions, would be desired for more accurate estimates of insulin secretion with genetic/pharmacological manipulation of islets.

Last, inspired by the unique phenotype of *Chop*-deleted β cells, we discovered that a GLP1-conjugated *Chop* ASO could partially recapitulate “ER remodeling” characterized by a reduced ER Ca^{2+} pool, thereby providing a promising therapeutic strategy for further pharmacological characterization and refinement to combat human T2D and fatty liver disease.

MATERIALS AND METHODS

Study design

The purpose of this study was to critically evaluate the metabolic consequence in mice of deleting *Chop* in β cells and subsequently to investigate whether GLP1-*Chop* ASO could also reduce liver TGs analogous to *Chop* βKO mice. For the first aim, we carried out the conditional Chop deletion model that was created by breeding a floxed *Ddit3* gene allele (15) with a RIP-CreERT transgene (16). In this model, β cell–specific Chop deletion is temporally controlled by TAM injections (referred to as *Chop* βKO mice; see Table 1 for breeding scheme). All available mice with predefined genotypes are included with no further selection. For the second aim, two widely used murine NAFLD models, namely, the male DIO-C57BL6/J model and the $Lpr^{db/db}$ model, were applied for GLP1-*Chop* ASO treatment. All HFD mice were males, to eliminate any potential confounding influences of gender differences, because females have been documented to be inconsistently responsive to DIO manipulation (17). All mice were randomly assigned to treatment groups, and all analyses were performed blinded to treatment conditions. The number of biologic replicates is specified in the figure legends. Sample size for each experiment including number of mice per group was initially based on historical data and was subsequently estimated by power analysis (with $\alpha = 0.05$ and power = 0.80; http://biomath.info/power/ttest.htm) to ensure adequate power for main conclusions.

Mouse diet and husbandry

Standard mouse diet (Teklad Global Irradiated Diet) and water were available ad libitum at all times, except for a 4- to 6-hour fasting period before IPGTT when indicated. For the HFD studies (45% fat in kcal%; OpenSource Diets), male mice from 2 to 3 litters were mixed and matched, with $n = 2$ to 4 mice per cage without genotype separation. Mice were only separated into individual cages for food intake measurement, when indicated. All procedures were performed by protocols and guidelines approved by the Institutional Animal Care and Use Committee (IACUC) at the Sanford Burnham Prebys (SBP) Medical Discovery Institute. For metabolic caging and body composition studies, animal use was approved by the IACUC at the University of California San Diego.

Generation and genotyping of *Chop*$^{Fe/Fe}$ (*Ddit3*$^{Fe/Fe}$) mice

Transgenic mice were generated in house and characterized as previously published (15). This line was donated to The Jackson Laboratory, with strain catalog no. 030816 ("*B6.Cg-Ddit3*$^{tm1.1Irt/J}$"). For genotyping of the mice carrying the floxed *Chop/Ddit3* allele, primers targeting the L83 element were used as described on the website: https://www.jax.org/strain/030816.

Breeding strategy to generate *Chop* βKO mice

Chop$^{Fe/Fe}$ mice were first bred with a *RIP-CreER* transgenic mouse (16), in which the fusion protein of Cre recombinase and a mutant human estrogen receptor (*ERT2*) is driven by the rat insulin II (Ins2) promoter to generate the *Chop*$^{+/Fe}$: *RIP-Cre* founders. The *Chop*$^{+/Fe}$: *RIP-Cre* mice were further bred with *Chop*$^{+/Fe}$ mice to generate littermates of the following genotypes: (i) *Chop*$^{Fe/Fe}$: *RIP-Cre,* (ii) *Chop*$^{+/Fe}$: *RIP-Cre*, and (iii) *Chop*$^{+/+}$: *RIP-Cre.* After TAM injections, the *Ddit3* loci specifically in the β cells became (i) *Chop*$^{Δ/Δ}$: *RIP-Cre,* (ii) *Chop*$^{+/Δ}$: *RIP-Cre,* and (iii) *Chop*$^{+/+}$: *RIP-Cre,* respectively. In selected experiments, *Chop*$^{-/-}$ mice were used (instead of *Chop*$^{+/Fe}$ mice) to breed with the *Chop*$^{+/Fe}$: *RIP-Cre* founder so that progeny of the following genotypes were generated: (i) *Chop*$^{Fe/-}$: *RIP-Cre* and (ii) *Chop*$^{+/-}$: *RIP-Cre.* After TAM injections, the *Ddit3* loci specifically in the β cells became (i) *Chop*$^{Δ/-}$: *RIP-Cre* and (ii) *Chop*$^{+/-}$: *RIP-Cre,* respectively. Refer to Table 1 for specific breeding schemes used for presented results.

Whole-transcriptome bioinformatics analysis

For RNA-Seq of islets, polyadenylate [poly(A)]–enriched RNAs extracted from three male mice were prepared for both genotypes, with the number (proportion) of successfully aligned reads from a sample ranging from 55 million to 80 million (>98% mapping rate). TopHat Splice-aware Aligner was used to align reads to the mouse reference genome (mm10) plus known splice junctions, created by ERANGE scripts and UCSC known genes (http://genome.ucsc.edu). Read counts were normalized to RPKM (reads per kilobase pair per million reads mapped) values for transcript abundance comparison. Trimmed mean of *M* (TMM) values were used for between-sample comparisons. For differential expression analysis, generalized linear model likelihood ratio tests were implemented in EdgeR software.

Targeted delivery of ASOs

For effects of *Chop* gene silencing in β cells, *Chop* gene–floxed mice (*B6.Cg-Ddit3*$^{tm1.1Irt/J}$; The Jackson Laboratory, catalog no. 030816) were treated twice with GLP1-Chop ASO, once every 5 to 7 days, by subcutaneous injections of PBS-diluted GLP1-ASO compounds in a volume of 0.2 ml per injection. GLP1-control ASO was administered to control littermate mice in parallel at the same time. A method describing the synthesis and characterization of the GLP1-ASO moiety can be found in the study of Ämmälä *et al.* (44). Three days after the second GLP1-ASO injection, mice were sacrificed for islet isolation and characterization.

For effects of GLP1-ASO dosing on liver TGs, two mouse models of NAFLD were tested. For the DIO model, male C57Bl6 mice received 10 weekly GLP1-ASOs (1 mg/kg per week of scrambled ASO or *Chop*) or unconjugated *Chop* ASO doses at (0.5 mg/kg per week), 12 weeks after 45% HFD initiation (a total of 22 weeks of HFD). For the *Lpr*$^{db/db}$ model, male *Lpr*$^{db/db}$ mice received eight weekly GLP1-ASO (3.2 mg/kg per week) or unconjugated *Chop* ASO (1.6 mg/kg per week) doses, starting from 5 weeks of age with standard diet (LabDiet no. 5008). Mice were sacrificed at the end of GLP1-ASO/ASO dosing. Liver TG and pancreas insulin content were measured and reported. More details of experimental procedures can be found in the Supplementary Materials.

Statistical analysis

All data subjected to parametric tests were normal according to Shapiro-Wilk using GraphPad's Prism software (version 9.0). Student's *t* test (two-sided) was used only when comparing two groups, with an α level of 0.05. Continuous variables, such as TG, glucose, and insulin concentrations, were compared using either a two-way RM-ANOVA or ordinary two-way ANOVA (Prism software) with an α level of 0.05. For two-way RM-ANOVA tests, time and genetics or compounds were assumed to be independent parameters. Bonferroni's multiple comparisons test was subsequently performed for comparison between individual groups (KO versus control group). Statistical significance was expressed as follows: n.s., not significant; *$P \leq 0.05$; **$P \leq 0.01$; ***$P < 0.001$; ****$P < 0.0001$. Statistical analysis details are provided in data files S1 to S4. Details of transcriptomic statistical analysis are provided in Supplementary Materials and Methods.

Supplementary Material

Refer to Web version on PubMed Central for supplementary material.

Acknowledgments:

The generation of a *Ddit3* gene–floxed mouse model was a collaborative effort with I. Tabas at Columbia University. J.-L. Li, F. Qi, and J. Yin at the SBP Applied Bioinformatics Core provided guidance and helpful discussion on the transcriptomic data analysis. G. Garcia at the SBP Histology Core facility provided technical assistance and helpful discussion on histology quantification methodology using an Aperio ScanScope FL instrument. Tissue analysis was facilitated by the SBP Histology Core at Lake Nona, with technical assistance from J. Shelley.

Funding:

R.J.K. is supported by NIH grants R01DK113171, R24DK110973, R37DK042394, and R01CA198103 and SBP NCI Cancer Center grant P30 CA030199. R.J.K. is a member of the UCSD DRC (P30 DK063491) and an adjunct professor in the Department of Pharmacology, UCSD. S.M.R. is supported by NIH grant R01DK126944 and ADA grant 1-19-JDF-012. A.R.S. is supported by NIH grants R01DK117551, R01DK125820, R01DK124496, and R01DK076906 and is a member of the UCSD DRC (P30 DK063491). L.S.S. is supported by NIH grant R01DK46409. C.L. is supported by NIH training grant T32DK007494 and is a member of the UCSD DRC. V.S.P. acknowledges support from an Upjohn Foundation postdoctoral fellowship.

REFERENCES AND NOTES

1. Centers for Disease Control and Prevention, National Diabetes Statistics Report (2017).
2. Weyer C, Funahashi T, Tanaka S, Hotta K, Matsuzawa Y, Pratley RE, Tataranni PA, Hypoadiponectinemia in obesity and type 2 diabetes: Close association with insulin resistance and hyperinsulinemia. J. Clin. Endocrinol. Metab 86, 1930–1935 (2001). [PubMed: 11344187]
3. Chon S, Gautier J-F, An update on the effect of incretin-based therapies on β-cell function and mass. Diabetes Metab. J 40, 99–114 (2016). [PubMed: 27126881]
4. Weyer C, Hanson RL, Tataranni PA, Bogardus C, Pratley RE, A high fasting plasma insulin concentration predicts type 2 diabetes independent of insulin resistance: Evidence for a pathogenic role of relative hyperinsulinemia. Diabetes 49, 2094–2101 (2000). [PubMed: 11118012]
5. Mehran AE, Templeman NM, Brigidi GS, Lim GE, Chu K-Y, Hu X, Botezelli JD, Asadi A, Hoffman BG, Kieffer TJ, Bamji SX, Clee SM, Johnson JD, Hyperinsulinemia drives diet-induced obesity independently of brain insulin production. Cell Metab. 16, 723–737 (2012). [PubMed: 23217255]
6. Templeman NM, Clee SM, Johnson JD, Suppression of hyperinsulinaemia in growing female mice provides long-term protection against obesity. Diabetologia 58, 2392–2402 (2015). [PubMed: 26155745]
7. Smith GI, Shankaran M, Yoshino M, Schweitzer GG, Chondronikola M, Beals JW, Okunade AL, Patterson BW, Nyangau E, Field T, Sirlin CB, Talukdar S, Hellerstein MK, Klein S, Insulin resistance drives hepatic de novo lipogenesis in nonalcoholic fatty liver disease. J. Clin. Invest 130, 1453–1460 (2020). [PubMed: 31805015]
8. Page MM, Skovsø S, Cen H, Chiu AP, Dionne DA, Hutchinson DF, Lim GE, Szabat M, Flibotte S, Sinha S, Nislow C, Rodrigues B, Johnson JD, Reducing insulin via conditional partial gene ablation in adults reverses diet-induced weight gain. FASEB J. 32, 1196–1206 (2018). [PubMed: 29122848]
9. Hassler JR, Scheuner DL, Wang S, Han J, Kodali VK, Li P, Nguyen J, George JS, Davis C, Wu SP, Bai Y, Sartor M, Cavalcoli J, Malhi H, Baudouin G, Zhang Y, Yates JR III, Itkin-Ansari P, Volkmann N, Kaufman RJ, The IRE1α/XBP1s pathway is essential for the glucose response and protection of β cells. PLOS Biol. 13, e1002277 (2015). [PubMed: 26469762]
10. Kutlu B, Burdick D, Baxter D, Rasschaert J, Flamez D, Eizirik DL, Welsh N, Goodman N, Hood L, Detailed transcriptome atlas of the pancreatic beta cell. BMC Med. Genomics 2, 3 (2009).
11. Szabat M, Page MM, Panzhinskiy E, Skovsø S, Mojibian M, Fernandez-Tajes J, Bruin JE, Bround MJ, Lee JTC, Xu EE, Taghizadeh F, O'Dwyer S, de Bunt M, Moon K-M, Sinha S, Han J, Fan Y, Lynn FC, Trucco M, Borchers CH, Foster LJ, Nislow C, Kieffer TJ, Johnson JD, Reduced insulin production relieves endoplasmic reticulum stress and induces β cell proliferation. Cell Metab. 23, 179–193 (2015). [PubMed: 26626461]
12. Song B, Scheuner D, Ron D, Pennathur S, Kaufman RJ, *Chop* deletion reduces oxidative stress, improves β cell function, and promotes cell survival in multiple mouse models of diabetes. J. Clin. Invest 118, 3378–3389 (2008). [PubMed: 18776938]
13. Maris M, Overbergh L, Gysemans C, Waget A, Cardozo AK, Verdrengh E, Cunha JP, Gotoh T, Cnop M, Eizirik DL, Burcelin R, Mathieu C, Deletion of C/EBP homologous protein (*Chop*) in C57Bl/6 mice dissociates obesity from insulin resistance. Diabetologia 55, 1167–1178 (2012). [PubMed: 22237685]
14. Satoh T, Abiru N, Kobayashi M, Zhou H, Nakamura K, Kuriya G, Nakamura H, Nagayama Y, Kawasaki E, Yamasaki H, Yu L, Eisenbarth GS, Araki E, Mori M, Oyadomari S, Eguchi K, CHOP

deletion does not impact the development of diabetes but suppresses the early production of insulin autoantibody in the NOD mouse. Apoptosis 16, 438–448 (2011). [PubMed: 21274633]

15. Zhou A-X, Wang X, Lin CS, Han J, Yong J, Nadolski MJ, Borén J, Kaufman RJ, Tabas I, C/EBP-homologous protein (CHOP) in vascular smooth muscle cells regulates their proliferation in aortic explants and atherosclerotic lesions. Circ. Res 116, 1736–1743 (2015). [PubMed: 25872946]
16. Dor Y, Brown J, Martinez OI, Melton DA, Adult pancreatic β-cells are formed by self-duplication rather than stem-cell differentiation. Nature 429, 41–46 (2004). [PubMed: 15129273]
17. Parks BW, Sallam T, Mehrabian M, Psychogios N, Hui ST, Norheim F, Castellani LW, Rau CD, Pan C, Phun J, Zhou Z, Yang W-P, Neuhaus I, Gargalovic PS, Kirchgessner TG, Graham M, Lee R, Tontonoz P, Gerszten RE, Hevener AL, Lusis AJ, Genetic architecture of insulin resistance in the mouse. Cell Metab. 21, 334–347 (2015). [PubMed: 25651185]
18. Bertolotti M, Lonardo A, Mussi C, Baldelli E, Pellegrini E, Ballestri S, Romagnoli D, Loria P, Nonalcoholic fatty liver disease and aging: Epidemiology to management. World J. Gastroenterol 20, 14185–14204 (2014). [PubMed: 25339806]
19. Frith J, Day CP, Henderson E, Burt AD, Newton JL, Non-alcoholic fatty liver disease in older people. Gerontology 55, 607–613 (2009). [PubMed: 19690397]
20. Koehler EM, Schouten JNL, Hansen BE, van Rooij FJA, Hofman A, Stricker BH, Janssen HLA, Prevalence and risk factors of non-alcoholic fatty liver disease in the elderly: Results from the Rotterdam study. J. Hepatol 57, 1305–1311 (2012). [PubMed: 22871499]
21. Ogrodnik M, Miwa S, Tchkonia T, Tiniakos D, Wilson CL, Lahat A, Day CP, Burt A, Palmer A, Anstee QM, Grellscheid SN, Hoeijmakers JHJ, Barnhoorn S, Mann DA, Bird TG, Vermeij WP, Kirkland JL, Passos JF, von Zglinicki T, Jurk D, Cellular senescence drives age-dependent hepatic steatosis. Nat. Commun 8, 15691 (2017). [PubMed: 28608850]
22. Perl S, Kushner JA, Buchholz BA, Meeker AK, Stein GM, Hsieh M, Kirby M, Pechhold S, Liu EH, Harlan DM, Tisdale JF, Significant human β-cell turnover is limited to the first three decades of life as determined by *in vivo* thymidine analog incorporation and radiocarbon dating. J. Clin. Endocrinol. Metab 95, E234–E239 (2010). [PubMed: 20660050]
23. Kushner JA, The role of aging upon beta cell turnover. J. Clin. Invest 123, 990–995 (2013). [PubMed: 23454762]
24. Teta M, Long SY, Wartschow LM, Rankin MM, Kushner JA, Very slow turnover of β-cells in aged adult mice. Diabetes 54, 2557–2567 (2005). [PubMed: 16123343]
25. Corkey BE, Banting lecture 2011: Hyperinsulinemia: Cause or consequence? Diabetes 61, 4–13 (2012). [PubMed: 22187369]
26. Templeman NM, Flibotte S, Chik JHL, Sinha S, Lim GE, Foster LJ, Nislow C, Johnson JD, Reduced circulating insulin enhances insulin sensitivity in old mice and extends lifespan. Cell Rep. 20, 451–463 (2017). [PubMed: 28700945]
27. Challet E, The circadian regulation of food intake. Nat. Rev. Endocrinol 15, 393–405 (2019). [PubMed: 31073218]
28. Han J, Back SH, Hur J, Lin Y-H, Gildersleeve R, Shan J, Yuan CL, Krokowski D, Wang S, Hatzoglou M, Kilberg MS, Sartor MA, Kaufman RJ, ER-stress-induced transcriptional regulation increases protein synthesis leading to cell death. Nat. Cell Biol 15, 481–490 (2013). [PubMed: 23624402]
29. Scheuner D, Vander Mierde D, Song B, Flamez D, Creemers JWM, Tsukamoto K, Ribick M, Schuit FC, Kaufman RJ, Control of mRNA translation preserves endoplasmic reticulum function in beta cells and maintains glucose homeostasis. Nat. Med 11, 757–764 (2005). [PubMed: 15980866]
30. Liu M, Li Y, Cavener D, Arvan P, Proinsulin disulfide maturation and misfolding in the endoplasmic reticulum. J. Biol. Chem 280, 13209–13212 (2005). [PubMed: 15705595]
31. Fan J, Wang Y, Liu L, Zhang H, Zhang F, Shi L, Yu M, Gao F, Xu Z, *cTAGE5* deletion in pancreatic β cells impairs proinsulin trafficking and insulin biogenesis in mice. J. Cell Biol 216, 4153–4164 (2017). [PubMed: 29133483]
32. Gold G, Gishizky ML, Grodsky GM, Evidence that glucose “marks” beta cells resulting in preferential release of newly synthesized insulin. Science 218, 56–58 (1982). [PubMed: 6181562]

33. Kaufman RJ, Malhotra JD, Calcium trafficking integrates endoplasmic reticulum function with mitochondrial bioenergetics. Biochim. Biophys.Acta 1843, 2233–2239 (2014). [PubMed: 24690484]
34. Yong J, Bischof H, Burgstaller S, Siirin M, Murphy A, Malli R, Kaufman RJ, Mitochondria supply ATP to the ER through a mechanism antagonized by cytosolic Ca^{2+}. eLife 8, e49682 (2019). [PubMed: 31498082]
35. Gilon P, Chae H-Y, Rutter GA, Ravier MA, Calcium signaling in pancreatic β-cells in health and in type 2 diabetes. Cell Calcium 56, 340–361 (2014). [PubMed: 25239387]
36. Sabourin J, Le Gal L, Saurwein L, Haefliger J-A, Raddatz E, Allagnat F, Store-operated Ca^{2+} entry mediated by Orai1 and TRPC1 participates to insulin secretion in rat β-cells. J. Biol. Chem 290, 30530–30539 (2015). [PubMed: 26494622]
37. Satin LS, Butler PC, Ha J, Sherman AS, Pulsatile insulin secretion, impaired glucose tolerance and type 2 diabetes. Mol. Aspects Med 42, 61–77 (2015). [PubMed: 25637831]
38. German MS, Moss LG, Rutter WJ, Regulation of insulin gene expression by glucose and calcium in transfected primary islet cultures. J. Biol. Chem 265, 22063–22066 (1990). [PubMed: 1979979]
39. Lawrence MC, Bhatt HS, Watterson JM, Easom RA, Regulation of insulin gene transcription by a Ca^{2+}-responsive pathway involving calcineurin and nuclear factor of activated T cells. Mol. Endocrinol 15, 1758–1767 (2001). [PubMed: 11579208]
40. Keller TL, Zocco D, Sundrud MS, Hendrick M, Edenius M, Yum J, Kim Y-J, Lee H-K, Cortese JF, Wirth DF, Dignam JD, Rao A, Yeo C-Y, Mazitschek R, Whitman M, Halofuginone and other febrifugine derivatives inhibit prolyl-tRNA synthetase. Nat. Chem. Biol 8, 311–317 (2012). [PubMed: 22327401]
41. Zhou H, Sun L, Yang X-L, Schimmel P, ATP-directed capture of bioactive herbal-based medicine on human tRNA synthetase. Nature 494, 121–124 (2013). [PubMed: 23263184]
42. Bruhat A, Jousse C, Carraro V, Reimold AM, Ferrara M, Fafournoux P, Amino acids control mammalian gene transcription: Activating transcription factor 2 is essential for the amino acid responsiveness of the *CHOP* promoter. Mol. Cell. Biol 20, 7192–7204 (2000). [PubMed: 10982836]
43. Heit JJ, Apelqvist ÅA, Gu X, Winslow MM, Neilson JR, Crabtree GR, Kim SK, Calcineurin/NFAT signalling regulates pancreatic β-cell growth and function. Nature 443, 345–349 (2006). [PubMed: 16988714]
44. Ämmälä C, Drury WJ III, Knerr L, Ahlstedt I, Stillemark-Billton P, Wennberg-Huldt C, Andersson E-M, Valeur E, Jansson-Löfmark R, Janzén D, Sundström L, Meuller J, Claesson J, Andersson P, Johansson C, Lee RG, Prakash TP, Seth PP, Monia BP, Andersson S, Targeted delivery of antisense oligonucleotides to pancreatic β-cells. Sci. Adv 4, eaat3386 (2018). [PubMed: 30345352]
45. Arunagiri A, Haataja L, Pottekat A, Pamenan F, Kim S, Zeltser LM, Paton AW, Paton JC, Tsai B, Itkin-Ansari P, Kaufman RJ, Liu M, Arvan P, Proinsulin misfolding is an early event in the progression to type 2 diabetes. eLife 8, e44532 (2019). [PubMed: 31184302]
46. Harding HP, Zeng H, Zhang Y, Jungries R, Chung P, Plesken H, Sabatini DD, Ron D, Diabetes mellitus and exocrine pancreatic dysfunction in *Perk*−/− mice reveals a role for translational control in secretory cell survival. Mol. Cell 7, 1153–1163 (2001). [PubMed: 11430819]
47. Scheuner D, Song B, McEwen E, Liu C, Laybutt R, Gillespie P, Saunders T, Bonner-Weir S, Kaufman RJ, Translational control is required for the unfolded protein response and in vivo glucose homeostasis. Mol. Cell 7, 1165–1176 (2001). [PubMed: 11430820]
48. Back SH, Scheuner D, Han J, Song B, Ribick M, Wang J, Gildersleeve RD, Pennathur S, Kaufman RJ, Translation attenuation through eIF2α phosphorylation prevents oxidative stress and maintains the differentiated state in beta cells. Cell Metab. 10, 13–26 (2009). [PubMed: 19583950]
49. Lee A-H, Heidtman K, Hotamisligil GS, Glimcher LH, Dual and opposing roles of the unfolded protein response regulated by IRE1α and XBP1 in proinsulin processing and insulin secretion. Proc. Natl. Acad. Sci. U.S.A 108, 8885–8890 (2011). [PubMed: 21555585]
50. Engin F, Yermalovich A, Nguyen T, Hummasti S, Fu W, Eizirik DL, Mathis D, Hotamisligil GS, Restoration of the unfolded protein response in pancreatic β cells protects mice against type 1 diabetes. Sci. Transl. Med 5, 211ra156 (2013).

51. Neel JV, Diabetes mellitus: A “thrifty” genotype rendered detrimental by “progress”? Am. J. Hum. Genet 14, 353–362 (1962). [PubMed: 13937884]
52. Smith GI, Polidori DC, Yoshino M, Kearney ML, Patterson BW, Mittendorfer B, Klein S, Influence of adiposity, insulin resistance, and intrahepatic triglyceride content on insulin kinetics. J. Clin. Invest 130, 3305–3314 (2020). [PubMed: 32191646]
53. Berglund ED, Li CY, Poffenberger G, Ayala JE, Fueger PT, Willis SE, Jewell MM, Powers AC, Wasserman DH, Glucose metabolism in vivo in four commonly used inbred mouse strains. Diabetes 57, 1790–1799 (2008). [PubMed: 18398139]
54. Montemurro C, Nomoto H, Pei L, Parekh VS, Vongbunyong KE, Vadrevu S, Gurlo T, Butler AE, Subramaniam R, Ritou E, Shirihai OS, Satin LS, Butler PC, Tudzarova S, IAPP toxicity activates HIF1α/PFKFB3 signaling delaying β-cell loss at the expense of β-cell function. Nat. Commun 10, 2679 (2019). [PubMed: 31213603]
55. Martin M, Cutadapt removes adapter sequences from high-throughput sequencing reads. EMBnet J. 17, 3 (2011).
56. Dobin A, Davis CA, Schlesinger F, Drenkow J, Zaleski C, Jha S, Batut P, Chaisson M, Gingeras TR, STAR: Ultrafast universal RNA-seq aligner. Bioinformatics 29, 15–21 (2013). [PubMed: 23104886]
57. Li B, Dewey CN, RSEM: Accurate transcript quantification from RNA-Seq data with or without a reference genome. BMC Bioinformatics 12, 323 (2011). [PubMed: 21816040]
58. Love MI, Huber W, Anders S, Moderated estimation of fold change and dispersion for RNA-seq data with DESeq2. Genome Biol. 15, 550 (2014). [PubMed: 25516281]
59. Jang I, Pottekat A, Poothong J, Yong J, Lagunas-Acosta J, Charbono A, Chen Z, Scheuner DL, Liu M, Itkin-Ansari P, Arvan P, Kaufman RJ, PDIA1/P4HB is required for efficient proinsulin maturation and ß cell health in response to diet induced obesity. eLife 8, e44528 (2019). [PubMed: 31184304]

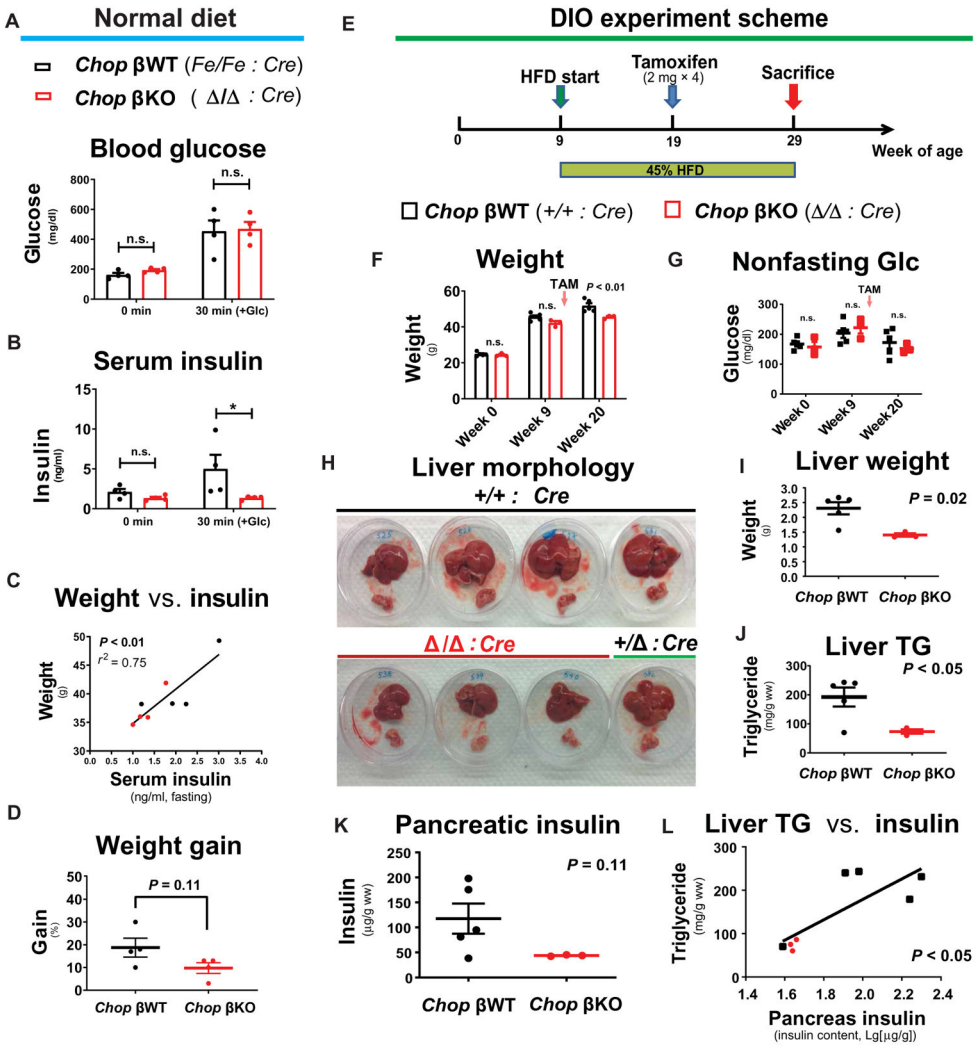

Fig. 1. β cell–specific *Chop* deletion reduces insulin in pancreata and in circulation and prevents liver TG accumulation in male DIO mice.

Under normal diet feeding, *Chop*-floxed ($n = 4$) and isogenic *Chop*-deleted ($n = 4$) littermates were tested 4 months after TAM injections. All mice were male. (**A** and **B**) After a glucose injection (1.5 mg/g body weight, intraperitoneally), glucose excursion showed no difference at 30 min after injection (A), whereas serum insulin concentrations were different at 30 min after glucose stimulation ($P < 0.05$, by Bonferroni's test after two-way RM-ANOVA) (B). (**C**) Correlation of the body weight of individual mice with fasting insulin ($P < 0.01$ by F test, $r^2 = 0.75$). (**D**) *Chop*-deleted mice cumulative weight gain 4 months after *Chop* deletion. $P = 0.11$ by two-tailed Student's t test. (**E**) *Chop*-floxed ($n = 3$) and congenic control littermates ($n = 5$, with 4 WT animals and 1 heterozygous animal) were fed with HFD (45% cal from fat) for 20 weeks before tissue harvest. Mice received TAM injections (four times every other day) at 10 weeks of HFD feeding to delete *Chop* via Cre recombinase. All mice were male. (**F**) Body weight after *Chop* deletion (week 20, $P < 0.01$) (10 weeks after *Chop* deletion by TAM). (**G**) Nonfasting blood glucose. (**H**) Appearance of fresh liver (top) and pancreas organs immediately after tissue dissection for all mice. (**I**) Liver weight of *Chop*-deleted animals (*Chop* βKO, after CreERT-mediated

Chop deletion) compared to WT and Het littermate control mice ($P = 0.02$). (**J**) Liver TGs in *Chop*-deleted mice compared to WT and Het littermate control mice ($P < 0.05$). (**K**) Pancreatic insulin in *Chop*-deleted mice compared to littermate control mice ($P = 0.11$). (**L**) Liver TG content correlation with pancreatic insulin content on a semi-log plot ($P < 0.05$). Data plotted are individual mice, with bar and whiskers representing means ± SEM.

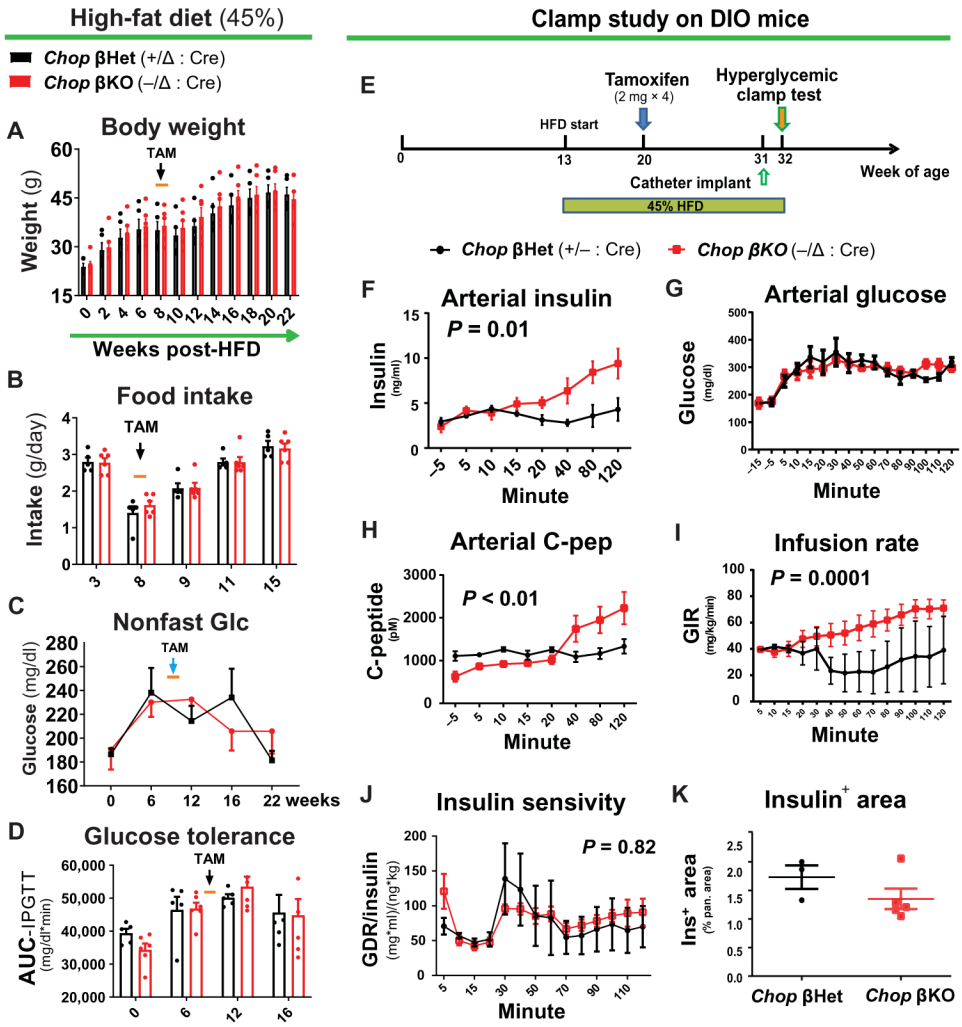

Fig. 2. β cell–specific *Chop* deletion improves insulin secretion after sustained glucose stimulation without altering glucose metabolism.

(**A** to **D**) Body weight (A), daily food intake (B), nonfasting blood glucose concentrations (C), and glucose excursion after an IPGTT test (D) in *Chop* βKO mice versus *Chop* βHet littermates fed 45% HFD for 22 weeks, starting at 9 weeks of age. (**E**) Experimental scheme for hyperglycemic clamp. *Chop*-floxed mice with congenic littermates were fed with HFD for 7 weeks before TAM injections (four times every other day). Mice were kept on HFD for another 12 weeks before the hyperglycemic clamp assay ($n = 8$ for *Chop* βKO and $n = 3$ for *Chop* βHet, both male and female mice were tested; see Table 2). (**F**) Insulin concentrations and C-peptide concentrations (H) in the arterial blood were measured by enzyme-linked immunosorbent assay (ELISA). (**G**) Hyperglycemic clamping was maintained at 300 mg/dl by continuous glucose infusion into the jugular vein via an implanted catheter. (**H**) Blood C-peptide concentrations are shown, as measured by ELISA. (**I**) Glucose infusion rates (GIRs). (**J**) Insulin sensitivity, defined as glucose disposal rate (GDR) divided by insulin plasma concentration. For (A) to (J), two-way RM-ANOVA was applied. (**K**) Area with insulin staining in pancreata dissected and fixed for histological analysis after the hyperglycemic

clamp assay. Data plotted are individual mice, with bar and whiskers representing means ± SEM.

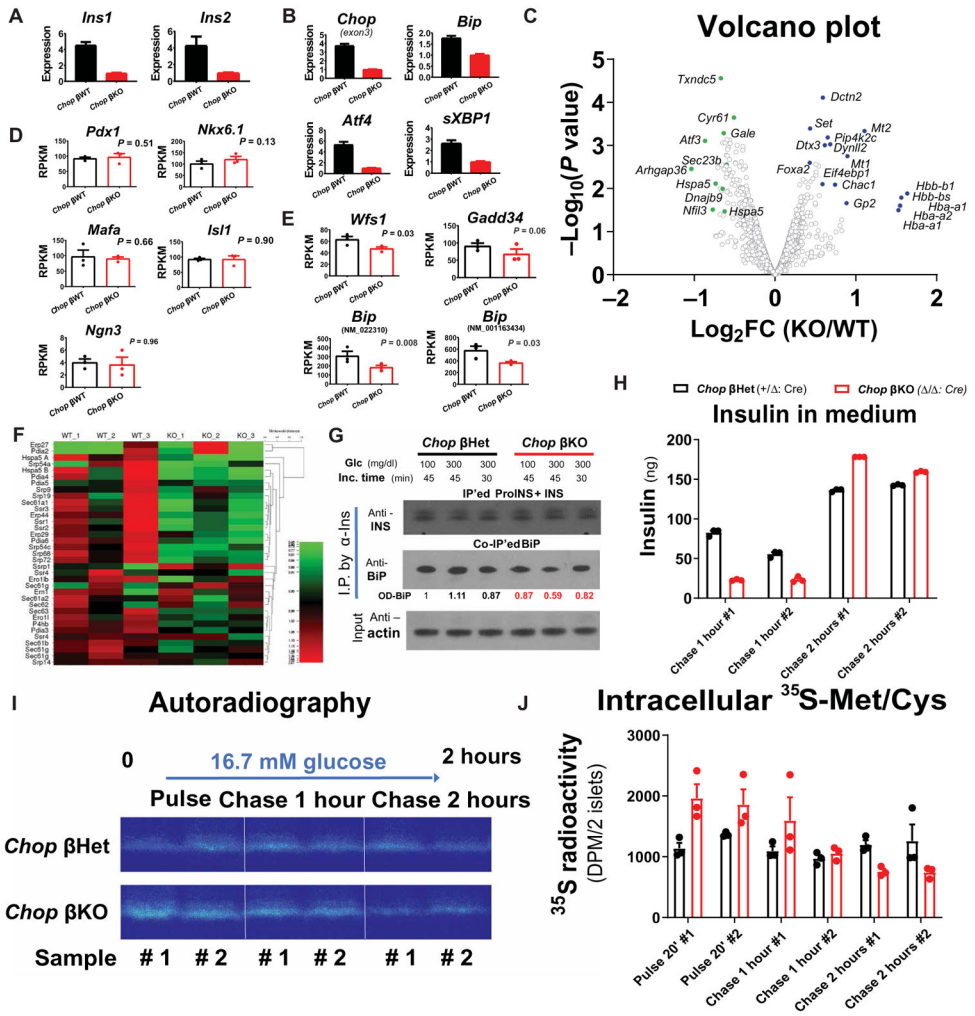

Fig. 3. *Chop* deletion reduces insulin-encoding mRNAs and ER stress in male DIO mice.

Chop βKO (*Fe/Fe: Cre*) and *Chop* βWT (+/+: *Cre*) congenic littermates ($n = 5$ per group, all male) were fed with HFD (45% cal from fat) for 45 weeks before TAM injections and were continued on HFD for another 8 weeks before islet isolation. (**A** and **B**) Abundance of transcripts encoding insulin (*Ins1* and *Ins2*) (A) and UPR genes (B). Experiment was repeated five times, with representative qRT-PCR results from one such experiment shown in (A) and (B). Islet RNA samples extracted from the same donors as in (A) and (B) were further analyzed by RNA-Seq ($n = 3$ per group). Transcriptomic profile analysis was performed using poly(A)-enriched mRNA samples isolated from the mice shown in (A) and (B) by next-generation sequencing. (**C**) Volcano plot of differential mRNA expression for both groups. Select genes with significant *P* values ($P < 0.05$) were labeled as green/blue dots to reflect down-/up-regulation as a result of *Chop* deletion. (**D** and **E**) RPKM values for important β cell lineage–determining genes, namely, *Pdx1/Nkx6.1/Mafa/Ngn3/Isl1* (D), and select UPR genes (E) were plotted, with *P* values indicated. (**F**) Heatmap for a group of select genes important for ER protein translation/translocation, with percentage change in expression shown. (**G**) Proinsulin-bound BiP protein was immunoprecipitated by anti-insulin co-IP in *Chop* βKO islets 6 weeks after TAM injection. Co-IP BiP was quantified by

optical density after Western blot. Islets from male donors (*Chop* βKO versus *Chop* βHet; *n* = 3 per group) were pooled and challenged with glucose after overnight culture. (**H**) Insulin ELISA assays showing insulin secretion dynamics with 16.7 mM glucose as stimulation. (**I**) Proinsulin (ProINS) processing in *Chop* βKO islets was monitored by pulse-chase assay and visualized by autoradiography. (**J**) Scintillation quantification showing retained ^{35}S radioactivity in the *Chop* βKO islets. *n* = 40 islets per condition.

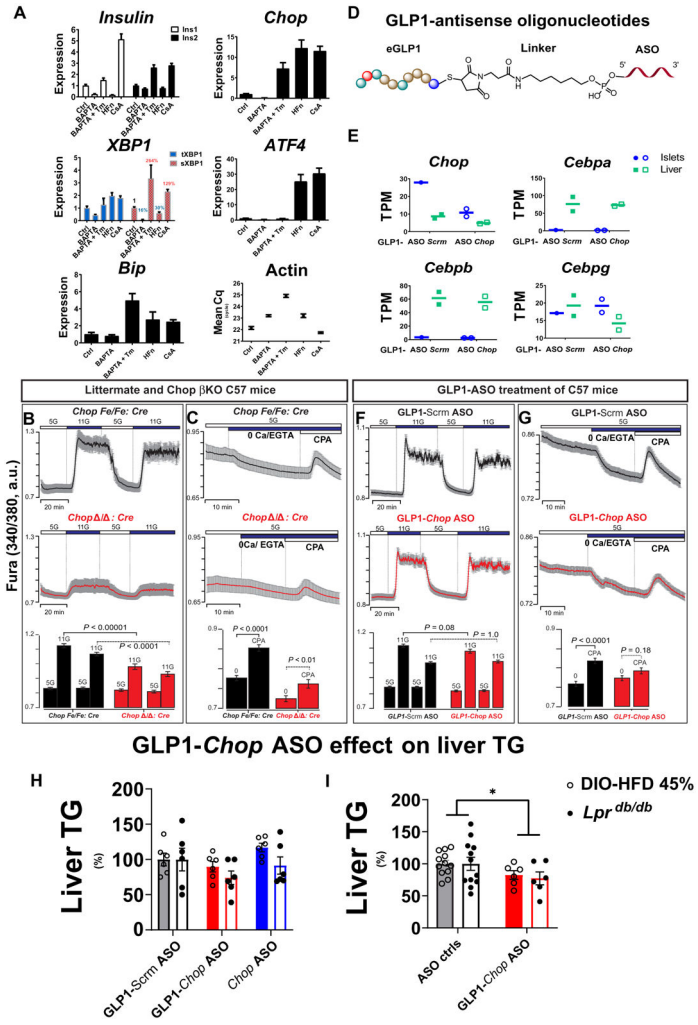

Fig. 4. ER stress up-regulates insulin-encoding mRNAs via ER Ca^{2+}, and targeting *Chop* decreases the ER Ca^{2+} pool.

(**A**) Islets isolated from male C57Bl6/J mice (*n* = 5) were pooled and divided into five groups after overnight culture, with ~120 islets per group. The islets were subsequently challenged with either dimethyl sulfoxide (“Ctrl”) or one of the following: 10 μM BAPTA acetoxymethyl ester (BAPTA-AM), 10 μM BAPTA-AM plus tunicamycin (Tm) (500 ng/ml), 50 nM halofuginone (HFn), or 200 nM cyclosporine A (CsA) for 18 hours before RNA extraction for qRT-PCR. Relative transcript abundance is summarized as bar graphs, using per-condition β-actin gene expression (“Mean Cq”) as a reference. (**B** and **C**) Cytosolic Ca^{2+} (B) and ER Ca^{2+} pools (C) in *Chop* βKO islets. Representative traces show intracellular Ca^{2+} signals (means ± 95% confidence interval) (*n* = 30 to 50 islets per group). Experiments were repeated three times using three pairs of control and βKO islets. Experimental conditions included physiological extracellular Ca^{2+} (2.56 mM), followed by extracellular Ca^{2+} removal and exposure to the reversible SERCA (sarco/endoplasmic reticulum Ca^{2+}-adenosine triphosphatase) pump inhibitor Cyclopiazonic acid (CPA) at 50 μM. Glucose [5 mM (“5G”) or 11 mM (“11G”)] was used for all experiments. Two-way ANOVA with post hoc Tukey multiple comparison tests was used for statistical analysis. a.u., arbitrary

units. (**D**) Illustration of GLP1-ASO chemical structure. (**E**) Effect of GLP1-ASO against *Chop* on *Chop* transcript abundance [expressed as transcripts per million (TPM)] in mouse islets. RNA extracted from the livers of the same mice served as internal controls for *Chop* RNA-Seq. Expression of additional C/EBP transcription factor family members is shown as controls. (**F** and **G**) Effect of GLP1-ASO treatment on glucose-induced cytosolic Ca^{2+} (F) and ER Ca^{2+} pools (G) in primary islets in vivo. Representative intracellular Ca^{2+} traces (means ± SEM) are shown (n = 30 to 50 islets per group). For (F) and (G), male and female *Ddit3*-floxed mice (without *RIP-CreER* transgene) were treated with GLP1-ASO before islet isolation. (**H** and **I**) GLP1-ASO dosing reduced liver TGs in two mouse models of NAFLD. Liver TGs were measured and reported as individual groups (H) or control groups versus GLP1-Chop ASO (I). n = 6 per group; $*P < 0.05$ for "GLP1-*Chop* ASO" effect. Solid bars, C57Bl6-DIO model; empty bars, $Lpr^{db/db}$ model. Two-way ANOVA with post hoc Tukey multiple comparison test was used for statistical analysis in (I).

Table 1.

Breeding strategies.

Fe, floxed gene allele; +, WT gene allele; −, KO gene allele.

Genotypes of breeding pair	Control littermate genotype (expected ratio for males)	*Chop*-βKO genotype (expected ratio for males)	Used in figures
Chop Fe/Fe : RIP-Cre* × *Chop Fe/Fe : 0	***Chop Fe/Fe : RIP-Cre* + *diluent injections*** (½ × ½ = 1/4)	***Chop Fe/Fe : RIP-Cre* + TAM injections** (½ × ½ = 1/4)	Figure 1, A to D
Chop Fe/+ : RIP-Cre* × *ChopFe/+:0	***Chop* +/+ : *RIP-Cre*** (½ × ½ × ¼ = 1/16)	***Chop Fe/Fe : RIP-Cre*** (½ × ½ × ¼ = 1/16)	Figure 1, F to L
Chop Fe/Fe : RIP-Cre* × *Chop* +/− : *0	***Chop Fe/+ : RIP-Cre*** (½ × ½ × ½ = 1/8)	***Chop Fe/− : RIP-Cre*** (½ × ½ × ½ = 1/8)	Figure 2, A to D
Chop* −/− : *RIP-Cre* × *Chop Fe/+: 0	***Chop* +/− : *RIP-Cre*** (½ × ½ × ½ = 1/8)	***Chop Fe/− : RIP-Cre*** (½ × ½ × ½ = 1/8)	Figure 2, F to K

Table 2.

Mice for hyperglycemic clamp study.

Data are displayed as means ± SEM.

Genotype	Male (*n*)	Female (*n*)	Total (*n*)	Body weight (g)	Fasting blood glucose (mg/dl)
Chop +/− : RIP-Cre	2	1	3	36.8 ± 1.2	173 ± 12
Chop Δ/− : RIP-Cre	6	2	8	39.6 ± 2.9[n.s., *]	197 ± 26[n.s., †]

[*] $P = 0.58$ by two-tailed *t* test, compared to control group.

[†] $P = 0.59$ by two-tailed *t* test, compared to control group.